



ISSN: 2723-9535

Available online at www.HighTechJournal.org

HighTech and Innovation Journal

Vol. 5, No. 1, March, 2024



The Development and Evaluation of Homogenously Weighted Moving Average Control Chart based on an Autoregressive Process

Rapin Sunthornwat ¹, Saowanit Sukparungsee ², Yupaporn Areepong ^{2*}

¹ Industrial Technology and Innovation Management Program, Faculty of Science and Technology, Pathumwan Institute of Technology 10330, Thailand.

² Department of Applied Statistics, Faculty of Applied Science, King Mongkut's University of Technology North Bangkok, Bangkok, 10800, Thailand.

Received 02 November 2023; Revised 14 February 2024; Accepted 21 February 2024; Published 01 March 2024

Abstract

This research aims to investigate a Homogenously Weighted Moving Average (HWMA) control chart for detecting minor and moderate shifts in the process mean. A mathematical model for the explicit formulae of the average run length (ARL) of the HWMA control chart based on the autoregressive (AR) process is presented. The efficacy of the HWMA control chart is evaluated based on the average run length, the standard deviation of run length (SDRL), and the median run length (MRL). As illustrations of the design and implementation of the HWMA control chart, numerical examples are provided. In numerous instances, a comparative analysis of the HWMA control chart relative to the Extended Exponentially Weighted Moving Average (Extended EWMA) and cumulative sum (CUSUM) control charts with mean process shifts is performed in detail. Additionally, the relative mean index (RMI), the average extra quadratic loss (AEQL), and the performance comparison index (PCI) are utilized to evaluate the performance of control charts. For various shift sizes, the HWMA control chart is superior to the Extended EWMA and CUSUM control charts. This study applies empirical data from the area of economics to validate the explicit formula of ARL values for the HWMA control chart.

Keywords: Integral Equation; Average Run Length; Autoregressive Process.

1. Introduction

Statistical process control (SPC) provides several benefits, including a reduction in defects, an increase in productivity, a reduction in waste, an increase in customer satisfaction, and an improvement in the overall performance of the process. It is extensively utilized across industries to maintain product quality and process consistency. A control chart is a statistical process control tool that continuously monitors and visually represents the performance of a process, product, or operation over time. Control charts are extensively utilized in manufacturing, healthcare, service industries, and virtually any setting where processes must be monitored and controlled. Various control charts are utilized to monitor and analyze different parts of a process.

The Shewhart control chart, which Shewhart [1] first proposed, the cumulative sum (CUSUM) control chart, which Page [2] first proposed, and the exponentially weighted moving average (EWMA) control chart, which Roberts [3] first published, are the three process control charts that are most frequently used. The EWMA and CUSUM control charts are designed to gather data over time to identify subtle adjustments in process parameters. In contrast, Shewhart control charts are mainly utilized for promptly detecting significant process shifts. Previous studies have indicated that the EWMA and CUSUM control charts exhibit superior performance compared to the Shewhart control chart in detecting

* Corresponding author: yupaporn.a@sci.kmutnb.ac.th

<https://dx.doi.org/10.28991/HIJ-2024-05-01-02>

➤ This is an open access article under the CC-BY license (<https://creativecommons.org/licenses/by/4.0/>).

© Authors retain all copyrights.

minor variations in the process [4, 5]. The Extended Exponentially Weighted Moving Average (Extended EWMA) control chart was introduced by Neveed et al. [6] to expand the conventional EWMA control chart. The purpose of this design is to identify changes in both the mean and the standard deviation of a process. A homogeneously weighted moving average (HWMA) control chart was recently proposed by Abbas [7] as a control charting statistic that gives the present and past samples a specific weight. The impact of non-normality on the HWMA control chart's performance is examined, and adjustments to the control chart's parameters may improve its performance against non-normality. Furthermore, Abbas [7] showed that the HWMA control chart outperformed the CUSUM and EWMA control charts in terms of effectiveness. In order to compare how successfully the charts identified process changes, the authors therefore aimed to offer an exact formula for the average run time of HWMA control charts. Riaz et al. [8] utilized Monte Carlo simulation to examine the performance of the HWMA control chart in zero and steady states at various shifts. The HWMA control chart is compared to the EWMA control chart with time-varying limits to conduct the comparative analysis. It has been determined that, for several shift sizes under zero state, the HWMA control chart is superior to the EWMA chart.

Control charts are often designed to be used in processes that have identically distributed (i.i.d.) data points for monitoring and analysis. Processes can, in fact, display autocorrelation, whereby prior observations impact the current data point. A type of autoregressive integrated moving average (ARIMA) model, AR models mix moving average and differencing components to address non-stationarity in the data. AR models are useful when there is a correlation between the values at various time points and the time series shows signs of autocorrelation. In this study, the criteria for choosing the ARIMA model with the lowest mean absolute percentage error (MAPE) and root mean square error (RMSE) were examined. Noise usually follows white noise; however, exponential white noise can also be followed by noise. As Fellag & Ibazizen [9] have done, a specific example of white noise with an exponential distribution will be considered.

The Average Run Length (ARL) is a measure of the expected or average number of samples that need to be collected before a control chart signals an out-of-control condition. The ARL is used to evaluate the performance and efficiency of a control chart in maintaining the process in an in-control state. The ARL has two essential components: ARL for the in-control state (ARL_0) refers to the average run length when the process is in the control condition. In an ideal scenario, the ARL for the in-control state should be relatively large, indicating that the chart does not frequently generate false alarms. ARL for out-of-control state (ARL_1) refers to the average run length when the process is out of control. It measures the average time required for the control chart to identify and signal a real problem or deviation from the intended process conditions. A small ARL_1 indicates that the control chart can rapidly detect a process change. Many approaches have been provided for evaluating the Average Run Length (ARL). For example, Champ & Rigdon [10] studied the Markov chain and integral equation approaches that are often used to evaluate the run length distribution of quality control charts to evaluate the cumulative sum (CUSUM) and the exponentially weighted moving average (EWMA) control charts. The product midpoint rule approximates the integral in the integral equation. Furthermore, Sukparungsee & Areepong [11] introduced an autoregressive model-based explicit analytical solution for the average run length of the EWMA control chart. They utilized the numerical integral equation method to compare the outcomes of the ARL. The use of explicit formulas for determining Average Run Length (ARL) values has yielded precise results and expedited computational processes. Consequently, many researchers have studied the derivation of Average Run Length (ARL) values using precise mathematical expressions.

Sunthornwat et al. [12] estimate the fractional differencing parameter and the optimal smoothing value for the EWMA control chart to assess the Average Run Length (ARL) and compare the analytical EWMA and CUSUM control charts. Peerajit et al. [13] recently proposed explicit formulas for the average run length (ARL) of the CUSUM chart for non-seasonal and seasonal ARFIMA models. The accuracy of explicit ARL was compared with the numerical integral equation (NIE) method based on the Gauss-Legendre quadrature rule. On a modified EWMA control chart for a first-order moving-average process with exponential white noise, Supharakonsakun [14] examined explicit formulations for both the one-sided and two-sided ARL. A comparison was made between the EWMA control chart's performance and the solution's accuracy as determined by the numerical integral equation method. Following this, Supharakonsakun [15] conducts an analysis on the efficacy of a modified EWMA chart in determining the precise average run length. The observations were obtained from a general-order moving average process accompanied by exponential white noise. Additionally, a comparison of the effectiveness of the EWMA and modified EWMA control charts is also presented. In the meanwhile, Phanyaem [16] introduced the explicit formula of the ARL for seasonal autoregressive with explanatory variables on the CUSUM chart. Subsequently, Petcharat [17] determined the average run length (ARL) for the cumulative sum (CUSUM) control chart by employing the Fredholm integral equation method and the SAR(P)L with trend process. The use of Banach's fixed point theorem guarantees the existence and uniqueness of the solution. Phanthuna et al. [18] have recently developed explicit analytical solutions for the ARL of a modified EWMA control chart with exponential white noise using a time series model with fractionality and integration. Peerajit and Areepong [19] presented the ARL of an autoregressive fractionally integrated process with exponential white noise using a modified EWMA control chart to detect variations in the mean process.

Furthermore, Silpakob et al. [20] created a modified exponentially weighted moving average (EWMA) control chart to determine a change in the mean process. They derived explicit formulas for both one-sided and two-sided ARL for autoregressive processes. The findings revealed that the performance of the newly modified EWMA control chart was superior to that of the conventional EWMA and the modified EWMA control charts. Peerajit [21] recently introduced an explicit formula for ARL for monitoring variations in the mean for the CUSUM control chart under the SFIMAX model. Karoon et al. [22] investigated the exact run length on a two-sided extended EWMA control chart that was autoregressive with a trend model to monitor the mean process. The effectiveness of the extended EWMA control chart for controlling process mean based on autocorrelated data was examined by Karoon et al. [23]. Peerajit [24] developed precise methods based on analytical integral equations to obtain the ARL. The proof of these formulas' existence and uniqueness relied on Banach's fixed-point theorem. This work examines the FIMAX model's CUSUM chart, which takes exogenous factors and a fractionally integrated moving average into account. The model assumes that there is an underlying exponential white noise. Using an analytical formula based on an integral equation, Peerajit [25] gave a precise estimation of the ARL for long-memory models in the same year. Examples of these models include fractionally integrated MAX processes (FIMAX) with exponential white noise operating on an EWMA control chart. Its efficacy was contrasted with the ARL determined by the widely recognized numerical integral equation (NIE) method. Sunthornwat et al.'s [26] recent study examined the HWMA control chart's explicit formula for the MAX model and contrasted its performance with that of the CUSUM control chart. When utilizing the EARL, ESDRL, and EMRL criteria, the HWMA control chart outperformed the CUSUM control chart. Therefore, the purpose of this study is to examine the HWMA control chart and evaluate its effectiveness in comparison to the CUSUM control chart and the Extended Exponentially Weighted Moving Average (Extended EWMA) control chart. The autoregressive model (AR(p)), a new model that will be used in numerous real-world applications, will be employed to apply this control chart. This study also identifies a new performance criterion that consists of PCI, AEQL, and RMI values.

Thus, the primary objective of this research is to evaluate the ARL formulas derived from the HWMA control chart for an autoregressive model under zero state and compare them to the ones utilized by the NIE method. In addition, the HWMA control chart is enlarged to allow for a comparison of the control chart's efficiency to the Extended EWMA and CUSUM control charts that underlie both simulated and real-world data for various shift sizes in the process mean. Then, the efficiency of the HWMA chart was calculated using the SDRL and MRL values. The outcomes of the HWMA control chart were verified using the performance measures, which include the performance comparison by index (PCI), average extra quadratic loss (AEQL), and relative mean index (RMI). Furthermore, the application used to illustrate this research is related to natural gas prices. Changes in the price of oil play an equal role in predicting the fundamental future movement of the exchange rate (Brahmasrene et al. [27]). Moreover, the oil price is a significant factor directly related to the economy. In this situation, control charts aim to identify patterns or movements in price behavior that may signal a change in market conditions. The remaining article is organized as follows: Section 2 describes the structure of the HWMA, Extended EWMA, and CUSUM processes and control charts. The Average Run Length is evaluated in Section 3 using explicit formulas and numerical integral equations. The fourth section of the report provides numerical results. Finally, concluding remarks are summarized in Section 5.

2. Process and Control Charts

This section includes the statistical scheme of the HWMA control chart, using data derived from the autoregressive model (AR(p)). Subsequently, the explicit formula derived from the analysis and the NIE method for calculating the Average Run Length (ARL) is shown.

2.1. The Autoregressive Process

There are stationary and non-stationary components in time-series data. The moving average (MA(q)), autoregressive (AR(p)), and autoregressive and moving average (ARMA(p,q)) models are the methods available for creating stationary time series. In this work, the autoregressive model, or AR(p) model, was studied. Equation 1 expresses the AR(p) as follows:

Definition 2.1 Let $\{Y_t, t = 1, 2, \dots\}$ be a sequence of AR(p) process given as in Equation 1;

$$Y_t = \phi_0 + \phi_1 Y_{t-1} + \phi_2 Y_{t-2} + \dots + \phi_p Y_{t-p} + \varepsilon_t \quad (1)$$

where ϕ_0 is a constant of model

ϕ_i is coefficients of autoregressive $i = 1, 2, \dots, p$.

ε_t is a exponential white noise process ($\varepsilon_t \sim \text{Exp}(\alpha)$)

The probability density function of ε_t is defined as $f(y, \alpha) = \frac{1}{\alpha} e^{-\frac{y}{\alpha}}$; $\alpha > 0$, and then initial values of the AR(p) model are $Y_0, Y_{-1}, \dots, Y_{1-p}$.

2.2. The HWMA Control Chart

Under the assumption that $\{H_t; t = 1, 2, 3, \dots\}$ is a sequence of i.i.d continuous random variables with a probability density function, the HWMA statistic is taken into consideration. Based on the AR(p) procedure, the HWMA statistic (H_t) is known as an upper HWMA statistic. H_t can be represented as in Equation 2 using the recursive formula.

$$H_t = \lambda Y_t + (1 - \lambda) \bar{Y}_{t-1}, \text{ for } t = 1, 2, 3, \dots \quad (2)$$

where Y_t is a sequence of the AR(p) process with exponential white noise, the constant value $\bar{Y}_0 = v$ is an initial value; $v \in [0, h]$ where h is an upper control limit of HWMA control chart.

The control limits of HWMA control chart consist of;

$$\begin{aligned} \text{Upper control limit: } UCL_t &= \begin{cases} \mu_0 + L_1 \sqrt{\frac{\sigma^2}{n} \lambda^2}, t = 1 \\ \mu_0 + L_1 \sqrt{\frac{\sigma^2}{n} [\lambda^2 + \frac{(1-\lambda)^2}{(t-1)}]}, t > 1 \end{cases} \\ \text{Lower control limit: } LCL_t &= \begin{cases} \mu_0 - L_1 \sqrt{\frac{\sigma^2}{n} \lambda^2}, t = 1 \\ \mu_0 - L_1 \sqrt{\frac{\sigma^2}{n} [\lambda^2 + \frac{(1-\lambda)^2}{(t-1)}]}, t > 1 \end{cases} \end{aligned}$$

where μ_0 is the target mean, σ is the process standard deviation and L_1 is the width of the control limits.

The HWMA stopping time (τ_h) is defined as;

$$\tau_h = \{t > 0; H_t \geq h\}, \text{ for } h > v.$$

where τ_h is the stopping time and h is UCL .

2.3. The Extended EWMA Control Chart

The Extended EWMA control chart was presented by Neveed et al. [6]. By giving more weight to recent data points, it is allowed to rapidly monitor and detect small to moderate changes in the mean process. The Extended EWMA statistic is given by:

$$E_t = \lambda_1 Y_t - \lambda_2 Y_{t-2} + (1 - \lambda_1 - \lambda_2) E_{t-1}, t = 1, 2, \dots \quad (3)$$

where λ_1 and λ_2 are exponential smoothing coefficient with $(0 < \lambda_1 \leq 1)$ and $(0 \leq \lambda_2 \leq \lambda_1)$ and the initial value is a constant, $E_0 = u$. The upper control limit (UCL) and lower control limit (LCL) of the Extended EWMA control chart are given by:

$$\begin{aligned} UCL &= \mu_0 + L_2 \sigma \sqrt{\frac{\lambda_1^2 + \lambda_2^2 - 2\lambda_1\lambda_2(1 - \lambda_1 + \lambda_2)}{2(\lambda_1 - \lambda_2) - (\lambda_1 - \lambda_2)^2}}, \\ LCL &= \mu_0 - L_2 \sigma \sqrt{\frac{\lambda_1^2 + \lambda_2^2 - 2\lambda_1\lambda_2(1 - \lambda_1 + \lambda_2)}{2(\lambda_1 - \lambda_2) - (\lambda_1 - \lambda_2)^2}}, \end{aligned}$$

where μ_0 is the target mean, σ is the process standard deviation, and L_2 is suitable control limit width.

The stopping time of the Extended EWMA control chart (τ_b) is given by:

$$\tau_b = \{t > 0; E_t \geq b\},$$

where τ_b is the stopping time and b is UCL .

2.4. The CUSUM Chart

For quality control, Page [2] produced the CUSUM control chart, which can be used to detect small changes in the process mean. Using the procedure described in Equation 4, the statistics of the CUSUM control chart can be expressed as follows:

$$C_t = \max(0, C_{t-1} + Y_t - \varpi), t = 1, 2, 3, \dots \quad (4)$$

where ϖ is a reference value, $C_0 = \varsigma$ is the initial value of CUSUM statistic; $\varsigma \in [0, s]$ and the CUSUM chart's stopping time is defined as $\tau_s = \{t > 0; C_t > s\}$ and s is UCL .

3. Evaluation of Average Run Length

3.1. Analytical Explicit Formulas of the ARL for AR(p) Model

From the recursion of HWMA statistics in Equation 2,

$$H_t = \lambda Y_t + (1 - \lambda) \bar{Y}_{t-1}$$

$$\text{and } Y_t = \phi_0 + \phi_1 Y_{t-1} + \phi_2 Y_{t-2} + \dots + \phi_p Y_{t-p} + \varepsilon_t$$

Consequently, the HWMA statistics can be displayed as:

$$H_t = \lambda(\phi_0 + \phi_1 Y_{t-1} + \phi_2 Y_{t-2} + \dots + \phi_p Y_{t-p} + \varepsilon_t) + (1 - \lambda) \bar{Y}_{t-1}$$

For $t=1$,

$$H_1 = \lambda(\phi_0 + \phi_1 Y_0 + \phi_2 Y_{-1} + \dots + \phi_p Y_{1-p} + \varepsilon_1) + (1 - \lambda) \bar{Y}_0$$

$$H_1 = \lambda(\phi_0 + \phi_1 Y_0 + \phi_2 Y_{-1} + \dots + \phi_p Y_{1-p}) + \lambda \varepsilon_1 + (1 - \lambda) \bar{Y}_0$$

$$\text{Let } B = \lambda(\phi_0 + \phi_1 Y_0 + \phi_2 Y_{-1} + \dots + \phi_p Y_{1-p})$$

Set $LCL=0$, $UCL=h$ for in control process and given $\bar{Y}_0 = v$ then:

$$0 < H_t < h$$

$$0 < \lambda B + (1 - \lambda) \bar{Y}_{t-1} < h$$

The zero state at $t = 1$ is considered, therefore $K(v)$ can be calculated as follows:

$$K(v) = 1 + \int_0^{\frac{h-(1-\lambda)v-B}{\lambda}} K(B + \lambda y + (1 - \lambda)v) f(y) dy \quad (5)$$

$$\text{Let } w = B + \lambda y + (1 - \lambda)v, \text{ then } dy = \frac{1}{\lambda} dw.$$

After changing the variable in Equation 5, the expression can be reformulated as:

$$K(v) = 1 + \frac{1}{\lambda} \int_0^h K(w) \frac{1}{\alpha} e^{-\frac{1}{\alpha} [\frac{w-(1-\lambda)v-B}{\lambda}]} dw$$

$$\text{Since we determine } \varepsilon_1 \sim \text{Exp}(\alpha) \text{ then } f(y) = \frac{1}{\alpha} e^{-\frac{y}{\alpha}}.$$

Thus:

$$K(v) = 1 + \frac{e^{\frac{(1-\lambda)v+B}{\alpha\lambda}}}{\alpha\lambda} \int_0^h K(w) \frac{1}{\alpha} e^{-\frac{w}{\alpha\lambda}} dw$$

$$\text{We setting that } C(v) = \frac{e^{\frac{(1-\lambda)v+B}{\alpha\lambda}}}{\alpha\lambda} \text{ and } P = \int_0^h K(w) \frac{1}{\alpha} e^{-\frac{w}{\alpha\lambda}} dw$$

$$\text{So that } K(v) = 1 + C(v)P. \quad (6)$$

$$\text{Since } P = \int_0^h K(v) \frac{1}{\alpha} e^{-\frac{w}{\alpha\lambda}} dw, \text{ we have;}$$

$$= \int_0^h (1 + C(w)P) e^{-\frac{w}{\alpha\lambda}} dw = \int_0^h e^{-\frac{w}{\alpha\lambda}} dw + \frac{P}{\alpha\lambda} \int_0^h e^{-\frac{w-\lambda w+B-w}{\alpha\lambda}} dw = \int_0^h e^{-\frac{w}{\alpha\lambda}} dw + \frac{P e^{\frac{B}{\alpha\lambda}}}{\alpha\lambda} \int_0^h e^{-\frac{\lambda w}{\alpha\lambda}} dw$$

$$P = -\alpha\lambda(e^{-\frac{h}{\alpha\lambda}} - 1) - \frac{P e^{\frac{B}{\alpha\lambda}}}{\lambda}(e^{-\frac{h}{\alpha}} - 1)$$

$$P = \frac{-\alpha\lambda[e^{-\frac{h}{\alpha\lambda}} - 1]}{[1 + \frac{e^{\frac{B}{\alpha\lambda}}}{\lambda}(e^{-\frac{h}{\alpha}} - 1)]}$$

Substituting P in (6), we obtain:

$$K(v) = 1 - \frac{e^{-\frac{h}{\alpha\lambda}} [e^{\frac{(1-\lambda)v+B}{\alpha\lambda}} - 1]}{1 + \frac{e^{\frac{B}{\alpha\lambda}}}{\lambda}(e^{-\frac{h}{\alpha}} - 1)}.$$

$$K(v) = 1 - \frac{e^{-\frac{h}{\alpha\lambda}} [e^{\frac{(1-\lambda)v+\lambda(\phi_0+\phi_1 Y_0+\phi_2 Y_{-1}+\dots+\phi_p Y_{1-p})}{\alpha\lambda}} - 1]}{1 + \frac{e^{\frac{\lambda(\phi_0+\phi_1 Y_0+\phi_2 Y_{-1}+\dots+\phi_p Y_{1-p})}{\alpha\lambda}}}{\lambda}(e^{-\frac{h}{\alpha}} - 1)}. \quad (7)$$

The in-control process ($\alpha = \alpha_0$), the ARL of the HWMA control chart can be expressed in the following formula:

$$ARL_0 = 1 - \frac{\frac{-h}{[e^{\alpha_0 \lambda} - 1]e} \frac{(1-\lambda)v + \lambda(\phi_0 + \phi_1 Y_0 + \phi_2 Y_{-1} + \dots + \phi_p Y_{1-p})}{\alpha_0 \lambda}}{\frac{\lambda(\phi_0 + \phi_1 Y_0 + \phi_2 Y_{-1} + \dots + \phi_p Y_{1-p})}{\alpha_0 \lambda} \frac{-h}{1 + \frac{e}{\lambda} (e^{\alpha_0} - 1)}}. \quad (8)$$

Additionally, the out-of-control process ($\alpha = \alpha_1$), the ARL of the HWMA control chart can be mathematically represented as follows:

$$ARL_1 = 1 - \frac{\frac{-h}{[e^{\alpha_1 \lambda} - 1]e} \frac{(1-\lambda)v + \lambda(\phi_0 + \phi_1 Y_0 + \phi_2 Y_{-1} + \dots + \phi_p Y_{1-p})}{\alpha_1 \lambda}}{\frac{\lambda(\phi_0 + \phi_1 Y_0 + \phi_2 Y_{-1} + \dots + \phi_p Y_{1-p})}{\alpha_1 \lambda} \frac{-h}{1 + \frac{e}{\lambda} (e^{\alpha_1} - 1)}}. \quad (9)$$

3.2. The Numerical Integral Equation Method

For an autoregressive model with exponential white noise, the analytical NIE technique for the ARL on the HWMA control chart is solved in this section. The ARL in this study is assessed using the Gauss-Legendre rule.

$$K(v) = 1 + \frac{1}{\lambda} \int_0^h K(w) f\left(\frac{w - (1-\lambda)v - \lambda(\phi_0 + \phi_1 Y_0 + \phi_2 Y_{-1} + \dots + \phi_p Y_{1-p})}{\lambda}\right) dw$$

The evaluation of an integral approximation is accomplished using the quadrature rule in the following:

$$\text{approach: } \int_0^h f(x) dx \approx \sum_{k=1}^n w_k f(a_k)$$

where a_k is a point and w_k is a weight that is defined by the quadrature rules.

By use the quadrature formula, we derive $\tilde{K}(a_h) = 1 + \frac{1}{\lambda} \sum_{k=1}^n w_k K(a_k) f\left(\frac{w - (1-\lambda)v - \lambda(\phi_0 + \phi_1 Y_0 + \phi_2 Y_{-1} + \dots + \phi_p Y_{1-p})}{\lambda}\right)$, $h = 1, 2, \dots, n$;

The system of n linear equations is as follows;

$$\tilde{K}(a_h) = 1 + \frac{1}{\lambda} \sum_{k=1}^n w_k K(a_k) f\left(\frac{w - (1-\lambda)v - \lambda(\phi_0 + \phi_1 Y_0 + \phi_2 Y_{-1} + \dots + \phi_p Y_{1-p})}{\lambda}\right), \quad h = 1, 2, \dots, n$$

$$\tilde{K}(a_1) = 1 + \frac{1}{\lambda} \sum_{k=1}^n w_k K(a_k) f\left(\frac{a_k - (1-\lambda)v - \lambda(\phi_0 + \phi_1 Y_0 + \phi_2 Y_{-1} + \dots + \phi_p Y_{1-p})}{\lambda}\right)$$

$$\tilde{K}(a_2) = 1 + \frac{1}{\lambda} \sum_{k=1}^n w_k K(a_k) f\left(\frac{a_k - (1-\lambda)v - \lambda(\phi_0 + \phi_1 Y_0 + \phi_2 Y_{-1} + \dots + \phi_p Y_{1-p})}{\lambda}\right)$$

⋮

$$\tilde{K}(a_n) = 1 + \frac{1}{\lambda} \sum_{k=1}^n w_k K(a_k) f\left(\frac{a_k - (1-\lambda)v - \lambda(\phi_0 + \phi_1 Y_0 + \phi_2 Y_{-1} + \dots + \phi_p Y_{1-p})}{\lambda}\right)$$

This system can be shown as:

$$K_{n \times 1} = (I_n - R_{n \times n})^{-1} 1_{n \times 1},$$

$$\text{where } K_{n \times 1} = \begin{bmatrix} \tilde{K}(a_1) \\ \tilde{K}(a_2) \\ \vdots \\ \tilde{K}(a_n) \end{bmatrix}, I_n = \text{diag}(1, 1, \dots, 1) \text{ and } 1_{n \times 1} = \begin{bmatrix} 1 \\ 1 \\ \vdots \\ 1 \end{bmatrix}.$$

Let $R_{n \times n}$ is a matrix and define the n to n^{th} as an element of the matrix R as follows;

$$[R_{hk}] \approx \frac{1}{\lambda} w_k f\left(\frac{w - (1-\lambda)v - \lambda(\phi_0 + \phi_1 Y_0 + \phi_2 Y_{-1} + \dots + \phi_p Y_{1-p})}{\lambda}\right)$$

If $(I - R)^{-1}$ exists, the numerical approximation for the integral equation corresponds to the term of the matrix,

$$K_{n \times 1} = (I_{n \times 1} - R_{n \times n})^{-1} 1_{n \times 1}$$

Eventually, we replace a_h by v , the numerical approximation of the integral for the function $K(v)$ represented as:

$$\tilde{K}(v) = 1 + \frac{1}{\lambda} \sum_{k=1}^n w_k K(a_k) f\left(\frac{a_k - (1-\lambda)v - \lambda(\phi_0 + \phi_1 Y_0 + \phi_2 Y_{-1} + \dots + \phi_p Y_{1-p})}{\lambda}\right) \quad (10)$$

3.3. The Existence and Uniqueness of Exact ARL Solution

The ARL formula's accuracy is theoretically verified by the Banach's Fixed-point Theorem, which guarantees that explicit formulations have a unique solution to the integral equation. Let V be an operation on the class of all continuous functions denoted by:

$$V(K(v)) = 1 + \frac{1}{\lambda} \int_0^h K(w) f\left(\frac{w-(1-\lambda)-\lambda(\phi_0+\phi_1Y_0+\phi_2Y_{-1}+\dots+\phi_pY_{1-p})}{\lambda}\right) dw \quad (11)$$

According to Banach's Fixed-point Theorem, if an operator V is a contraction, and then the fixed-point equation $V(K(v)) = K(v)$ has a unique solution. The following Theorem can be used to show that the equation in Equation 9 exists and has a unique solution.

Theorem 2. Banach's Fixed-point Theorem

Let (X, d) defined on a complete metric space and $V: X \rightarrow X$ satisfies the conditions of a contraction mapping with contraction constant $0 \leq \eta < 1$ such that $\|V(K_1) - V(K_2)\| \leq \eta \|K_1 - K_2\|, \forall K_1, K_2 \in X$. Then there exists a unique $K(\cdot) \in X$ such that $V(K(v)) = K(v)$, i.e., a unique fixed-point in X .

Proof of Theorem 2. Let V defined in (9) is a contraction mapping for $K_1, K_2 \in F[0, h]$, such that $\|V(K_1) - V(K_2)\| \leq \eta \|K_1 - K_2\|, \forall K_1, K_2 \in F[0, h]$ with $0 \leq \eta < 1$ under the norm

$$\|K\|_\infty = \sup_{v \in [0, h]} |K(v)|, \text{ so}$$

$$\begin{aligned} \|V(K_1) - V(K_2)\|_\infty &= \sup_{v \in [0, h]} \left| \frac{1}{\alpha\lambda} e^{\frac{(1-\lambda)v+\lambda(\phi_0+\phi_1Y_0+\phi_2Y_{-1}+\dots+\phi_pY_{1-p})}{\alpha\lambda}} \int_0^h (K_1(w) - K_2(w)) e^{-\frac{w}{\alpha\lambda}} dw \right| \\ &= \|K_1 - K_2\|_\infty \sup_{v \in [0, h]} \left| e^{\frac{(1-\lambda)v+\lambda(\phi_0+\phi_1Y_0+\phi_2Y_{-1}+\dots+\phi_pY_{1-p})}{\alpha\lambda}} \right| \left| 1 - e^{-\frac{h}{\alpha\lambda}} \right| \leq \eta \|K_1 - K_2\|_\infty \end{aligned}$$

$$\text{where } \eta = \sup_{v \in [0, h]} \left| e^{\frac{(1-\lambda)v+\lambda(\phi_0+\phi_1Y_0+\phi_2Y_{-1}+\dots+\phi_pY_{1-p})}{\alpha\lambda}} \right| \left| 1 - e^{-\frac{h}{\alpha\lambda}} \right|; \eta \in [0, 1).$$

3.4. The Performance Measurement

This section presents a simulation analysis comparing the NIE approach and explicit formulae' accuracy for the ARL of the AR(p) process on the HWMA control chart. The accuracy of the ARL values is compared with the percentage accuracy which can be obtained from

$$\%Accuracy = 100 - \left| \frac{K(v) - \tilde{K}(v)}{K(v)} \right| \times 100\% \quad (12)$$

Further, the efficacy of control charts in identifying out-of-control conditions is investigated using the Standard Deviation Run Length (SDRL) and Median Run Length (MRL) (Fonseca et al. [28]). The SDRL and MRL for the process under control are calculated as follows.

$$ARL_0 = \frac{1}{\alpha}, SDRL_0 = \sqrt{\frac{1-\alpha}{\alpha^2}}, MRL_0 = \frac{\log(0.5)}{\log(1-\alpha)}, \quad (13)$$

where α represents type I error. In this investigation, ARL_0 was fixed at 370, and it can be calculated by dividing $SDRL_0$ and MRL_0 by Equation 13 to yield values of approximately 370 and 256, respectively. $SDRL_1$ and MRL_1 are calculated differently for out-of-control situations by substituting α with β , where β represents type II error.

The efficacy of the control chart in detecting various types of process variations can be evaluated, and informed decisions about its performance. A control chart with the lowest ARL_1 , $SDRL_1$, and MRL_1 values is considered to have the best performance for rapidly identifying shifts in the process mean. Additionally, the performance efficiency of the HWMA control chart is compared with the Extended EWMA and CUSUM control charts by using the relative mean index (RMI) [29]. If the RMI is a small value, this control chart will have a quick and robust performance for detecting shifts. RMI is defined as:

$$RMI(c) = \frac{1}{n} \sum_{i=1}^n \left[\frac{ARL_i(c) - ARL_i(s)}{ARL_i(s)} \right] \quad (14)$$

where $ARL_i(c)$ is denoted the ARL of the control chart for the shift size of row i , while the smallest ARL among all control charts for the same shift size is represented by $ARL_i(s)$. Furthermore, the performance metrics can be employed to evaluate the effectiveness of a control chart under different changes $\delta_{max/min}$.

Moreover, the average extra quadratic loss (AEQL) may refer to the average extra loss incurred due to an out-of-control condition. During out-of-control periods, it could be calculated as the average difference between the observed values and the target or desired values. The calculation for AEQL is as follows [30]:

$$AEQL = \frac{1}{\Delta} \sum_{\delta_i = \delta_{min}}^{\delta_{max}} (\delta_i^2 \times ARL(\delta_i)) \quad (15)$$

where δ represents the particular change in the process, and Δ represents the sum of number of divisions from δ_{min} to δ_{max} . In this study, $\Delta = 9$ is determined from δ_{min} to δ_{max} . The control chart with the lowest AEQL values perform the best. Additionally, the performance comparison index (PCI) is a measurement used to compare the performance of

different control charts. The PCI measurement is the ratio between the AEQL of the control chart and the most efficient control chart, which is shown as the lowest AEQL. The mathematical formula for the PCI is:

$$PCI = \frac{AEQL}{AEQL_{lowest}} \quad (16)$$

3.5. The ARL Procedure for Analytical Results

This section will outline the procedures for calculating the ARL value using the explicit formula and the NIE method. When the process is in-control, $\alpha = \alpha_0$ is given to the exponential white noise parameter. And $\alpha_1 = (1 + \delta)\alpha_0$ is set when the process goes out of control. The computation of ARL involved in comparing ARL values from both methods are as follows and also shown in Figure 1:

Step 1: Determining the parameters of control chart and AR(p) process:

- Set the exponential white noise (α_0) and smoothing parameters for the in-control process.
- Set the initial values for the AR(p) process and the HWMA statistic.
- Determine suitable values for ARL_0 and the shift sizes(δ).

Step 2: Calculating the upper control limit (h) that yields the desired ARL for the control process by using Equation 8.

Step 3: Calculating ARL for the in-control process:

- Calculate ARL_0 by using Equation 8 when given the upper control limit (h) from Step 1.
- Calculate the value of ARL_0 via the explicit formula by using Equation 8.
- Determine the value of ARL_0 using the NIE approach by using Equation 10.
- Adjust the value of h to correspond with the targeted ARL_0 value.

Step 4: Calculating ARL for the out-of-control process:

- Calculate ARL_1 for various shift sizes and $\alpha_1 = (1 + \delta)\alpha_0$ by using Equation 9 and the value of h from Step.1
- Approximate ARL_1 via the NIE method by using Equation 10.

Step 5: Comparison ARL:

- Compare the ARL values obtained using the explicit formula in Equation 9 and NIE method in Equation 10.

Step 6: Comparison the performance of HWMA with EEWMA and CUSUM control charts.

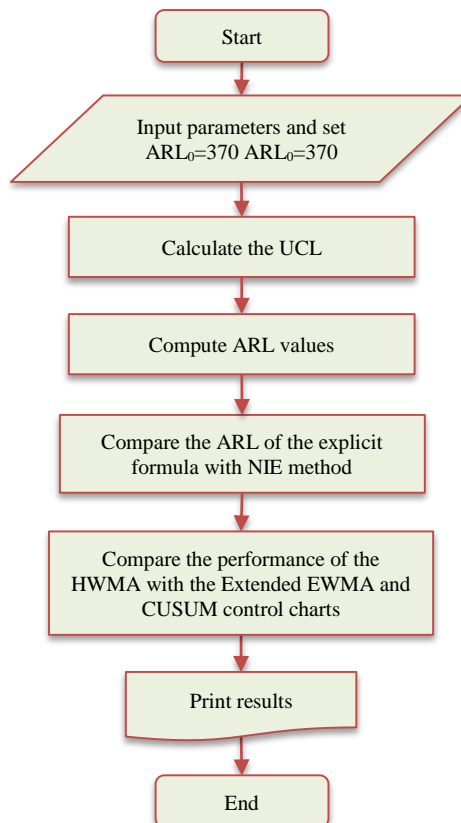


Figure 1. The process of the methodology

4. Results and Discussions

This section will present two main points: firstly, a comparison of the accuracy between the ARL explicit formula and the approximate ARL by NIE method for the AR(p) process on the HWMA control chart with various change levels; and secondly, a comparison of the performance of the HWMA control chart with the EWMA and CUSUM control charts in detecting changes in process means. ARL should be sufficiently large to support the in-control process when the under-study process is operating in an in-control process to avoid false alarms from occurring regularly. ARL_1 should be small for the out-of-control process to allow quick shift detection. A minimized ARL_1 value indicates a more effective control chart.

4.1. The Simulated Results

We consider the change in the process mean and process standard deviation subject to the changes in the exponential white noise parameter $\alpha_1 = (1 + \delta)\alpha_0$. Here, the shift sizes(δ) take the values 0.004, 0.008, 0.01, 0.04, 0.08, 0.10, and 0.40. Furthermore, the evaluation of the control charts' capacity to identify unusual shifts is conducted by varying the smoothing parameter values for $ARL_0 = 370$. The main insights regarding the outcomes are expanded in the following:

1. In Table 1, the control limits of HWMA control chart with AR(1), AR(2), and AR(3) processes are provided. The control limits were obtained after setting $\lambda = 0.01, 0.015, 0.02, 0.025, 0.03, 0.10, 0.15$ in-control process parameter $\alpha_0 = 1$. For example, in the case of AR(2) process given $\phi_0 = 0.01, \lambda = 0.01$, and $ARL_0 = 370$ the control limit is equal to 0.0073234.

Table 1. Control limits of HWMA control chart with AR processes

Models	Coefficients								
	ϕ_0	ϕ_1	ϕ_2	ϕ_3	$\lambda = 0.01$	$\lambda = 0.015$	$\lambda = 0.02$	$\lambda = 0.025$	$\lambda = 0.03$
AR(1)	0.01	0.1			0.0089552	0.0134816	0.0180257	0.0225896	0.0271740
AR(2)	0.01	0.1	0.2		0.0073234	0.0110215	0.0147309	0.0184533	0.0221891
AR(3)	0.01	0.1	0.2	0.3	0.0054177	0.0081506	0.0108890	0.0136343	0.0163869
AR(1)	0.01	-0.1			0.0109530	0.0164957	0.0220661	0.0276667	0.0332983
AR(2)	0.01	-0.1	-0.2		0.0133999	0.0201910	0.0270250	0.0339048	0.0408317
AR(3)	0.01	-0.1	-0.2	-0.3	0.0181425	0.0273652	0.0366698	0.0460603	0.0555391
	ϕ_0	ϕ_1	ϕ_2	ϕ_3	$\lambda = 0.10$	$\lambda = 0.15$	$\lambda = 0.20$	$\lambda = 0.25$	$\lambda = 0.30$
AR(1)	0.01	0.1			0.0936550	0.1439970	0.1970060	0.2529770	0.3122650
AR(2)	0.01	0.1	0.2		0.0760033	0.1162925	0.1582710	0.2020860	0.2479060
AR(3)	0.01	0.1	0.2	0.3	0.0557332	0.0848140	0.1147650	0.1456390	0.1774947
AR(1)	0.01	-0.1			0.1156515	0.1789200	0.2464580	0.3188850	0.3969650
AR(2)	0.01	-0.1	-0.2		0.1431980	0.2233075	0.3103940	0.4057850	0.5112400
AR(3)	0.01	-0.1	-0.2	-0.3	0.1986260	0.3150140	0.4467470	0.5984990	0.7774610

2. The comparison of the ARL_1 values produced by the numerical ARL methods and the explicit formula on the HWMA control chart for the AR(2) model with differing choice of λ with $\phi_0 = 0.01, ARL_0 = 370$ is shown in Tables 2 and 3. The ARL results were obtained after setting $\lambda = 0.01, 0.02, 0.03$ in Table 2 and $\lambda = 0.1, 0.2, 0.3$ in Table 3. The results indicate that the ARL are extremely similar and that the percentage accuracy is equal to 100 when both approaches are computed based on accuracy percentage. Nonetheless, the explicit formula's CPU time of about 0.001 is less than that of the NIE technique, which is about 1.6 seconds. In addition, it is found that when the λ value increases, the ARL value decreases at the same level of change. Furthermore, the SDRL and MRL values were the same direction as the ARL values.

Table 2. ARL results of explicit formulas and NIE method with AR(2) process for different choices of λ with $\phi_0 = 0.01, ARL_0 = 370$

λ	Coefficients of process			Methods	Shift size (δ)						
	ϕ_1	ϕ_2	b		0.004	0.008	0.01	0.04	0.08	0.1	0.4
0.01	0.1	0.2	0.0073234	Explicit	184.0047	122.3969	104.8452	33.29889	17.48924	14.15958	3.954241
				CPU _{Exp}	(<0.001)	(<0.001)	(<0.001)	(<0.001)	(<0.001)	(<0.001)	(<0.001)
				NIE	184.0047	122.3969	104.8452	33.29890	17.48924	14.15958	3.954240
				CPU _{NIE}	(1.609)	(1.625)	(1.641)	(1.609)	(1.641)	(1.609)	(1.625)
				% Acc	100.00	100.00	100.00	100.00	100.00	100.00	100.00
		-0.2	0.010953	Explicit	203.8752	140.6707	121.7941	40.46458	21.46985	17.41639	4.833761
				CPU _{Exp}	(<0.001)	(<0.001)	(<0.001)	(<0.001)	(<0.001)	(<0.001)	(<0.001)
				NIE	203.8753	140.6708	121.7941	40.46460	21.46985	17.41639	4.833760
				CPU _{NIE}	(1.625)	(1.625)	(1.609)	(1.625)	(1.625)	(1.594)	(1.610)
				% Acc	100.00	100.00	100.00	100.00	100.00	100.00	100.00
	0.2	0.2	0.0066231	Explicit	179.9503	118.8366	101.5852	31.98378	16.76081	13.56267	3.788305
				CPU _{Exp}	(<0.001)	(<0.001)	(<0.001)	(<0.001)	(<0.001)	(<0.001)	(<0.001)
				NIE	179.9504	118.8366	101.5852	31.98378	16.76081	13.56267	3.788310
				CPU _{NIE}	(1.641)	(1.594)	(1.609)	(1.609)	(1.625)	(1.610)	(1.593)
				% Acc	100.00	100.00	100.00	100.00	100.00	100.00	100.00
		-0.2	0.0099036	Explicit	198.2067	135.2958	116.7679	38.27715	20.25324	16.42226	4.571254
				CPU _{Exp}	(<0.001)	(<0.001)	(<0.001)	(<0.001)	(<0.001)	(<0.001)	(<0.001)
				NIE	198.2068	135.2958	116.7679	38.27716	20.25325	16.42227	4.571250
				CPU _{NIE}	(1.610)	(1.594)	(1.594)	(1.594)	(1.625)	(1.625)	(1.625)
				% Acc	100.00	100.00	100.00	100.00	100.00	100.00	100.00
0.02	0.1	0.2	0.0147309	Explicit	139.8667	86.42654	72.62748	21.83289	11.64208	9.534070	3.088052
				CPU _{Exp}	(<0.001)	(<0.001)	(<0.001)	(<0.001)	(<0.001)	(<0.001)	(<0.001)
				NIE	139.8667	86.42655	72.62749	21.83289	11.64208	9.534070	3.088050
				CPU _{NIE}	(1.594)	(1.578)	(1.610)	(1.640)	(1.656)	(1.641)	(1.594)
				% Acc	100.00	100.00	100.00	100.00	100.00	100.00	100.00
		-0.2	0.0220662	Explicit	159.4424	101.7907	86.27203	26.73764	14.31027	11.71729	3.719865
				CPU _{Exp}	(<0.001)	(<0.001)	(<0.001)	(<0.001)	(<0.001)	(<0.001)	(<0.001)
				NIE	159.4425	101.7907	86.27207	26.73765	14.31028	11.71729	3.719866
				CPU _{NIE}	(1.609)	(1.609)	(1.625)	(1.641)	(1.609)	(1.640)	(1.625)
				% Acc	100.00	100.00	100.00	100.00	100.00	100.00	100.00
	0.2	0.2	0.0133184	Explicit	136.0627	83.54507	70.09196	20.94726	11.15933	9.138001	2.969554
				CPU _{Exp}	(<0.001)	(<0.001)	(<0.001)	(<0.001)	(<0.001)	(<0.001)	(<0.001)
				NIE	136.0627	83.54509	70.09197	20.94726	11.15933	9.138000	2.969554
				CPU _{NIE}	(1.593)	(1.625)	(1.609)	(1.625)	(1.625)	(1.609)	(1.640)
				% Acc	100.00	100.00	100.00	100.00	100.00	100.00	100.00
		-0.2	0.0199428	Explicit	153.6162	97.13764	82.12037	25.22385	13.48867	11.04640	3.530567
				CPU _{Exp}	(<0.001)	(<0.001)	(<0.001)	(<0.001)	(<0.001)	(<0.001)	(<0.001)
				NIE	153.6163	97.13768	82.12040	25.22386	13.48868	11.04640	3.530570
				CPU _{NIE}	(1.641)	(1.609)	(1.640)	(1.641)	(1.625)	(1.609)	(1.625)
				% Acc	100.00	100.00	100.00	100.00	100.00	100.00	100.00

0.1	0.2	0.0221892	Explicit	126.2992	76.41419	63.89156	18.99983	10.21095	8.400650	2.865010
			CPU _{Exp}	(<0.001)	(<0.001)	(<0.001)	(<0.001)	(<0.001)	(<0.001)	(<0.001)
			NIE	126.2993	76.41420	63.89157	18.99984	10.21095	8.400651	2.865008
			CPU _{NIE}	(1.625)	(1.594)	(1.625)	(1.625)	(1.641)	(1.610)	(1.609)
			% Acc	100.00	100.00	100.00	100.00	100.00	100.00	100.00
	-0.2	0.0332983	Explicit	145.4102	90.77216	76.49872	23.35693	12.57243	10.33406	3.437505
			CPU _{Exp}	(<0.001)	(<0.001)	(<0.001)	(<0.001)	(<0.001)	(<0.001)	(<0.001)
			NIE	145.4103	90.77220	76.49875	23.35694	12.57244	10.33406	3.437510
			CPU _{NIE}	(1.610)	(1.625)	(1.625)	(1.640)	(1.609)	(1.625)	(1.625)
			% Acc	100.00	100.00	100.00	100.00	100.00	100.00	100.00
	0.2	0.0200545	Explicit	122.5142	73.71040	61.54534	18.21682	9.785970	8.051790	2.758150
			CPU _{Exp}	(<0.001)	(<0.001)	(<0.001)	(<0.001)	(<0.001)	(<0.001)	(<0.001)
			NIE	122.5143	73.71041	61.54535	18.21682	9.785970	8.051790	2.758150
			CPU _{NIE}	(1.625)	(1.609)	(1.609)	(1.625)	(1.625)	(1.594)	(1.578)
			% Acc	100.00	100.00	100.00	100.00	100.00	100.00	100.00
	-0.2	0.0300784	Explicit	139.7719	86.42875	72.662080	22.00802	11.84285	9.737945	3.265459
			CPU _{Exp}	(<0.001)	(<0.001)	(<0.001)	(<0.001)	(<0.001)	(<0.001)	(<0.001)
			NIE	139.7719	86.42878	72.66210	22.00803	11.84286	9.737950	3.265459
			CPU _{NIE}	(1.625)	(1.609)	(1.641)	(1.625)	(1.610)	(1.594)	(1.625)
			% Acc	100.00	100.00	100.00	100.00	100.00	100.00	100.00

Note: The numerical results in parentheses are computational times in second.

Table 3. ARL results of explicit formulas and NIE method with AR(2) process for different choices of λ with $\phi_0 = 0.01, ARL_0 = 370$

λ	Coefficients of process			Methods	Shift size (δ)						
	ϕ_1	ϕ_2	b		0.004	0.008	0.01	0.04	0.08	0.1	0.4
0.1	0.2	0.0760033		Explicit	110.7426	65.49227	54.47828	16.07262	8.741300	7.237580	2.636631
				CPU _{Exp}	(<0.001)	(<0.001)	(<0.001)	(<0.001)	(<0.001)	(<0.001)	(<0.001)
				NIE	110.7426	65.49229	54.47830	16.07262	8.741300	7.237585	2.636630
				CPU _{NIE}	(1.594)	(1.625)	(1.625)	(1.610)	(1.625)	(1.625)	(1.641)
				% Acc	100.00	100.00	100.00	100.00	100.00	100.00	100.00
	-0.2	0.1156515		Explicit	131.2544	80.14457	67.18359	20.27702	11.00570	9.090510	3.192092
				CPU _{Exp}	(<0.001)	(<0.001)	(<0.001)	(<0.001)	(<0.001)	(<0.001)	(<0.001)
				NIE	131.2546	80.14464	67.18364	20.27703	11.00570	9.090510	3.192090
				CPU _{NIE}	(1.562)	(1.578)	(1.640)	(1.609)	(1.625)	(1.610)	(1.656)
				% Acc	100.00	100.00	100.00	100.00	100.00	100.00	100.00
0.1	0.2	0.0685125		Explicit	107.0277	62.91628	52.26109	15.35365	8.352197	6.918040	2.536803
				CPU _{Exp}	(<0.001)	(<0.001)	(<0.001)	(<0.001)	(<0.001)	(<0.001)	(<0.001)
				NIE	107.0277	62.91630	52.26110	15.35366	8.352200	6.918044	2.536803
				CPU _{NIE}	(1.609)	(1.625)	(1.625)	(1.609)	(1.594)	(1.641)	(1.625)
				% Acc	100.00	100.00	100.00	100.00	100.00	100.00	100.00
	-0.2	0.104043		Explicit	125.0088	75.57754	63.20157	18.93942	10.28736	8.504056	3.021285
				CPU _{Exp}	(<0.001)	(<0.001)	(<0.001)	(<0.001)	(<0.001)	(<0.001)	(<0.001)
				NIE	125.0089	75.57759	63.20161	18.93943	10.28736	8.504058	3.021290
				CPU _{NIE}	(1.593)	(1.656)	(1.625)	(1.610)	(1.625)	(1.594)	(1.609)
				% Acc	100.00	100.00	100.00	100.00	100.00	100.00	100.00

0.1	0.2	0.158271	Explicit	111.4606	65.97207	54.88944	16.21152	8.822032	7.306020	2.664663
			CPU _{Exp}	(<0.001)	(<0.001)	(<0.001)	(<0.001)	(<0.001)	(<0.001)	(<0.001)
			NIE	111.4608	65.97213	65.97213	16.21153	8.822034	7.306020	2.664660
			CPU _{NIE}	(1.625)	(1.594)	(1.610)	(1.578)	(1.641)	(1.610)	(1.609)
			% Acc	100.00	100.00	100.00	100.00	100.00	100.00	100.00
	-0.2	0.246458	Explicit	136.1859	83.80362	70.38534	21.36064	11.58393	9.560768	3.322547
			CPU _{Exp}	(<0.001)	(<0.001)	(<0.001)	(<0.001)	(<0.001)	(<0.001)	(<0.001)
			NIE	136.1865	83.80387	70.38552	21.36066	11.58393	9.560774	3.322547
			CPU _{NIE}	(1.641)	(1.609)	(1.593)	(1.625)	(1.640)	(1.594)	(1.609)
			% Acc	100.00	100.00	100.00	100.00	100.00	100.00	100.00
	0.2	0.142075	Explicit	107.1431	62.99641	52.33168	15.38787	8.378500	6.942550	2.553330
			CPU _{Exp}	(<0.001)	(<0.001)	(<0.001)	(<0.001)	(<0.001)	(<0.001)	(<0.001)
			NIE	107.1432	62.99645	52.33171	15.38787	8.378500	6.942554	2.553330
			CPU _{NIE}	(1.625)	(1.625)	(1.609)	(1.610)	(1.594)	(1.594)	(1.625)
			% Acc	100.00	100.00	100.00	100.00	100.00	100.00	100.00
	-0.2	0.22019	Explicit	128.3554	78.02164	65.33161	19.65383	10.67113	8.817430	3.112634
			CPU _{Exp}	(<0.001)	(<0.001)	(<0.001)	(<0.001)	(<0.001)	(<0.001)	(<0.001)
			NIE	128.3558	78.02180	65.33173	19.65384	10.67113	8.817434	3.112635
			CPU _{NIE}	(1.578)	(1.610)	(1.610)	(1.640)	(1.610)	(1.625)	(1.625)
			% Acc	100.00	100.00	100.00	100.00	100.00	100.00	100.00
0.2	0.2	0.247906	Explicit	115.0221	68.45685	57.02951	16.89262	9.178866	7.594535	2.740620
			CPU _{Exp}	(<0.001)	(<0.001)	(<0.001)	(<0.001)	(<0.001)	(<0.001)	(<0.001)
			NIE	115.0225	68.45698	57.02960	16.89263	9.178870	7.594540	2.740618
			CPU _{NIE}	(1.610)	(1.609)	(1.593)	(1.609)	(1.610)	(1.625)	(1.625)
			% Acc	100.00	100.00	100.00	100.00	100.00	100.00	100.00
	-0.2	0.396965	Explicit	145.4781	90.86855	76.60295	23.48986	12.70819	10.46934	3.553795
			CPU _{Exp}	(<0.001)	(<0.001)	(<0.001)	(<0.001)	(<0.001)	(<0.001)	(<0.001)
			NIE	145.4797	90.86921	76.60342	23.48991	12.70821	10.46935	3.553800
			CPU _{NIE}	(1.625)	(1.594)	(1.610)	(1.594)	(1.610)	(1.625)	(1.593)
			% Acc	100.00	100.00	100.00	100.00	100.00	100.00	100.00
	0.2	0.221471	Explicit	109.9660	64.94908	54.00954	15.91745	8.655680	7.166671	2.612544
			CPU _{Exp}	(<0.001)	(<0.001)	(<0.001)	(<0.001)	(<0.001)	(<0.001)	(<0.001)
			NIE	109.9662	64.94917	54.00960	15.91746	15.91746	7.166670	2.612540
			CPU _{NIE}	(1.610)	(1.609)	(1.579)	(1.625)	(1.609)	(1.610)	(1.609)
			% Acc	100.00	100.00	100.00	100.00	100.00	100.00	100.00
	-0.2	0.351603	Explicit	135.5077	83.31025	69.95301	21.19887	11.48539	9.475818	3.282781
			CPU _{Exp}	(<0.001)	(<0.001)	(<0.001)	(<0.001)	(<0.001)	(<0.001)	(<0.001)
			NIE	135.5088	83.31067	69.95331	21.1989	11.48540	9.475825	3.282782
			CPU _{NIE}	(1.594)	(1.593)	(1.579)	(1.594)	(1.593)	(1.625)	(1.609)
			% Acc	100.00	100.00	100.00	100.00	100.00	100.00	100.00

Note: The numerical results in parentheses are computational times in seconds.

3. In Tables 4, the ARL of HWMA control chart for AR(2) model using explicit formula against Extended EWMA and CUSUM control charts for different choices of λ with $\phi_0 = 0.01, \phi_1 = 0.1, \phi_2 = 0.2, ARL_0 = 370$ are compared. For example, for δ change to 0.01, for $\lambda = 0.01$ ARL decreases from 370 to 14.15958, for $\lambda = 0.10$ ARL decreases from 370 to 7.237717 and for $\lambda = 0.2$ ARL decreases from 370 to 7.306020. Furthermore, it was discovered that HWMA control charts were the fastest at detecting changes at all change levels when compared to Extended EWMA and CUSUM control charts. The outcomes of Table 5's comparison of the efficacy of control charts with the AR(3) model are in the same direction as those of Table 4. Moreover, when the RMI and AEQL values from Tables 4 and 5 are considered, the HWMA control chart has the lowest RMI and AEQL values. Additionally, the PCI value of the HWMA control chart also equals 1, verifying that the HWMA control chart has the highest performance.

Table 4. The ARL of HWMA control chart for AR(2) using explicit formula against Extended EWMA and CUSUM control charts given $\phi_0 = 0.01, \phi_1 = 0.1, \phi_2 = 0.2$ and $\alpha_0 = 1$.

λ		$\lambda_1=0.01$			$\lambda_1=0.1$			$\lambda_1=0.2$		
δ	Control Chart	HWMA	EWMA $\lambda_2=0.005$	CUSUM $a=4$	HWMA	EEWMA $\lambda_2=0.05$	CUSUM $a=4$	HWMA	EEWMA $\lambda_2=0.1$	CUSUM $a=4$
	UCL	0.0073234	0.0120775	1.432	0.0760035	0.1245097	1.432	0.158271	0.257305	1.432
0.000	ARL ₀	370.467	370.0205	370.348	370.4595	370.8249	370.348	370.7615	370.9559	370.348
	SDRL ₀	369.9666	369.5201	369.8477	369.9591	370.3246	369.8477	370.2612	370.4556	369.8477
	MRL ₀	256.4414	256.1319	256.3589	256.4362	256.6895	256.3589	256.6456	256.7803	256.3589
0.002	ARL ₁	245.8854	268.1707	365.981	170.2343	196.8122	365.981	171.0674	197.6334	365.981
	SDRL ₁	245.3849	267.6702	365.4807	169.7336	196.3115	365.4807	170.5667	197.1328	365.4807
	MRL ₁	170.0879	185.5349	253.332	117.6505	136.0729	253.332	118.228	136.6422	253.332
0.004	ARL ₁	184.0047	210.2855	361.681	110.7811	134.2153	361.681	111.4606	134.9623	361.681
	SDRL ₁	183.504	209.7849	361.1807	110.2799	133.7144	361.1807	110.9595	134.4614	361.1807
	MRL ₁	127.1954	145.412	250.3514	76.44048	92.68395	250.3514	76.91153	93.20173	250.3514
0.008	ARL ₁	122.3969	146.8759	353.283	65.50561	82.32452	353.283	65.97207	82.87974	353.283
	SDRL ₁	121.8959	146.375	352.7826	65.00368	81.82299	352.7826	65.47016	82.37822	352.7826
	MRL ₁	84.492	101.4596	244.5304	45.05757	56.71573	244.5304	45.3809	57.10058	244.5304
0.01	ARL ₁	104.8452	127.6324	349.182	54.48747	69.08969	349.182	54.88944	69.57705	349.182
	SDRL ₁	104.344	127.1315	348.6816	53.98515	68.58787	348.6816	54.38714	69.07524	348.6816
	MRL ₁	72.32603	88.12104	241.6878	37.42019	47.54191	241.6878	37.69882	47.87973	241.6878
0.02	ARL ₁	61.06833	77.11843	329.604	29.87616	38.60833	329.604	30.11616	38.91001	329.604
	SDRL ₁	60.56627	76.6168	329.1036	29.3719	38.10505	329.1036	29.61194	38.40675	329.1036
	MRL ₁	41.98182	53.1071	228.1173	20.36004	26.41317	228.1173	20.52641	26.62229	228.1173
0.04	ARL ₁	33.29889	43.06284	294.655	16.07336	20.93302	294.655	16.21152	21.10816	294.655
	SDRL ₁	32.79508	42.5599	294.1546	15.56533	20.4269	294.1546	15.70357	20.6021	294.1546
	MRL ₁	22.7327	29.50096	203.8925	10.79092	14.16026	203.8925	10.88672	14.28169	203.8925
0.08	ARL ₁	17.48924	22.91338	238.42	8.7415	11.36602	238.42	8.822032	11.46673	238.42
	SDRL ₁	16.98188	22.40781	237.9195	8.226319	10.85451	237.9195	8.306998	10.95533	237.9195
	MRL ₁	11.77264	15.5332	164.9133	5.705557	7.526435	164.9133	5.761445	7.59629	164.9133
0.10	ARL ₁	14.15958	18.59339	215.703	7.237717	9.387661	215.703	7.30602	9.472397	215.703
	SDRL ₁	13.65043	18.08648	215.2024	6.719139	8.873585	215.2024	6.787629	8.958455	215.2024
	MRL ₁	9.463871	12.53819	149.1671	4.661644	6.153952	149.1671	4.709074	6.212749	149.1671
0.20	ARL ₁	7.359294	9.67329	137.436	4.188452	5.356299	137.436	4.231024	5.407585	137.436
	SDRL ₁	6.841047	9.159653	136.9351	3.654406	4.830491	136.9351	3.697369	4.882048	136.9351
	MRL ₁	4.746068	6.352138	94.91638	2.540903	3.354202	94.91638	2.570592	3.389876	94.91638
RMI		0	0	0.2383	6.9398	6.9398	0.2626	14.1634	0	0.262
AEQL		0.0720	0.072	0.094	1.0943	1.0943	0.0494	1.0943	0.0388	0.0499
PCI		1	1	1.3056	15.2017	15.2017	1.2873	28.4947	1	1.2867

Table 5. The ARL of HWMA control chart for AR(3) using explicit formula against Extended EWMA and CUSUM control charts given $\phi_0 = 0.01$, $\phi_1 = 0.1$, $\phi_2 = 0.2$, $\phi_3 = 0.3$ and $\alpha_0 = 1$.

λ		$\lambda_1 = 0.01$				$\lambda_1 = 0.1$			$\lambda_1 = 0.2$	
δ	Control Chart	HWMA	EEWMA $\lambda_2 = 0.005$	CUSUM a=4	HWMA	EEWMA $\lambda_2 = 0.05$	CUSUM a=4	HWMA	EEWMA $\lambda_2 = 0.1$	CUSUM a=4
	UCL	0.0054177	0.008935	1.129	0.0557333	0.091465	1.129	0.114765	0.187328	1.129
0.000	ARL ₀	370.59	370.2827	370.641	370.7671	370.5314	370.641	370.7544	370.617	370.641
	SDRL ₀	370.0897	369.7824	370.1407	370.2668	370.0311	370.1407	370.2541	370.1167	370.1407
	MRL ₀	256.5267	256.3137	256.562	256.6495	256.4861	256.562	256.6407	256.5454	256.562
0.002	ARL ₁	235.5205	253.8489	366.279	157.6979	177.7128	366.279	156.8015	176.4717	366.279
	SDRL ₁	235.02	253.3484	365.7787	157.1971	177.2121	365.7787	156.3007	175.971	365.7787
	MRL ₁	162.9036	175.6079	253.5385	108.9609	122.8342	253.5385	108.3396	121.974	253.5385
0.004	ARL ₁	172.5957	193.124	361.986	100.4174	117.1638	361.986	99.7031	116.0915	361.986
	SDRL ₁	172.095	192.6233	361.4857	99.91614	116.6627	361.4857	99.20184	115.5905	361.4857
	MRL ₁	119.2873	133.5165	250.5628	69.25688	80.8647	250.5628	68.76177	80.12145	250.5628
0.008	ARL ₁	112.4729	130.6312	353.599	58.43439	69.97283	353.599	57.96549	69.2239	353.599
	SDRL ₁	111.9718	130.1302	353.0986	57.93223	69.47103	353.0986	57.46332	68.72208	353.0986
	MRL ₁	77.61318	90.19961	244.7494	40.15606	48.15406	244.7494	39.83104	47.63494	244.7494
0.01	ARL ₁	95.7844	112.4411	349.503	48.42291	58.3434	349.503	48.02647	57.69983	349.503
	SDRL ₁	95.28309	111.94	349.0026	47.9203	57.84124	349.0026	47.52384	57.19765	349.0026
	MRL ₁	66.04551	77.59117	241.9103	33.21642	40.09299	241.9103	32.94162	39.64689	241.9103
0.02	ARL ₁	54.97847	66.29976	329.949	26.34255	32.1576	329.949	26.12474	31.78825	329.949
	SDRL ₁	54.47618	65.79786	329.4486	25.83771	31.65365	329.4486	25.61986	31.28426	329.4486
	MRL ₁	37.76054	45.60804	228.3565	17.91046	21.94155	228.3565	17.75946	21.68552	228.3565
0.04	ARL ₁	29.68477	36.44274	295.039	14.12756	17.34352	295.039	14.01952	17.15178	295.039
	SDRL ₁	29.18049	35.93926	294.5386	13.61838	16.8361	294.5386	13.51027	16.64427	294.5386
	MRL ₁	20.22736	24.912	204.1587	9.441665	11.67161	204.1587	9.366743	11.53866	204.1587
0.08	ARL ₁	15.49015	19.23176	238.851	7.68889	9.435694	238.851	7.64145	9.345016	238.851
	SDRL ₁	14.98181	18.72508	238.3505	7.171481	8.921694	238.3505	7.123925	8.830872	238.3505
	MRL ₁	10.38653	12.98078	165.2121	4.974914	6.187281	165.2121	4.941977	6.124362	165.2121
0.10	ARL ₁	12.5214	15.58568	216.146	6.373	7.810113	216.146	6.338045	7.740622	216.146
	SDRL ₁	12.011	15.07739	215.6454	5.851677	7.292993	215.6454	5.816594	7.223338	215.6454
	MRL ₁	8.327792	10.45276	149.4741	4.060999	5.059073	149.4741	4.036711	5.010829	149.4741
0.20	ARL ₁	6.48884	8.110357	137.877	3.711732	4.508561	137.877	3.70154	4.481941	137.877
	SDRL ₁	5.967931	7.593914	137.3761	3.172574	3.977256	137.3761	3.162255	3.950425	137.3761
	MRL ₁	4.141485	5.267499	95.22206	2.208101	2.764053	95.22206	2.200978	2.745504	95.22206
	RMI	0	0	0.1891	7.924	0	0.2013	16.1925	0	0.1979
	AEQL	0.0638	0.0638	0.0791	1.0971	0.0339	0.0414	1.0971	0.0338	0.041
	PCL	1	1	1.2405	17.206	1	1.2193	32.3349	1	1.2153

4.2. The Real-World Datasets

In this particular section, the explicit formulas for the average run length (ARL) of an autoregressive (AR) process on the EWMA control chart are applied and compared with the performance of the extended EWMA and cumulative sum (CUSUM) control charts. Following the subsequent steps, the ARL formula has been implemented using actual data.

1. To estimate parameters from a dataset, it is necessary to include an autoregressive model of order p (AR(p)).
2. To estimate the parameter of residuals that follow an exponential distribution.
3. By utilizing the parameter values obtained from the previous two steps, we can calculate the Average Run Length (ARL) values in Equations 8 and 9.

4. To perform a performance comparison, the ARL value obtained from 3. was compared with the Extended EWMA and CUSUM control charts.
5. To identify variations in the mean of a process, it is necessary to calculate the upper control limit (UCL) using the formula provided in Equation 4. Subsequently, the control chart statistics should be computed using actual data, and these statistics should be plotted on a graph to visualize any deviations.

In the context of practical application, this study is carried out utilizing daily data of natural gas prices from January 2, 2023 to April 4, 2023. The models were fitted using the SPSS program. The suitable model for dataset that correspond to AR(1) and AR(2) models is identified, and the relevant parameters are displayed in Table 6. As a result, the AR(1) model shows the lowest RMSE and MAPE values, implying that the AR(1) is the best model. The coefficient parameters for AR(1) are derived as shown in Table 6: $\hat{\phi}_1 = 0.999$. As shown in Table 7, the mean parameter of exponential white noise was then determined using the one-sample Kolmogorov-Smirnov test. The in-control parameter is equal to 0.1223. The parameter of this prediction model, can be assigned as $\hat{Y}_t = 0.999Y_{t-1}$.

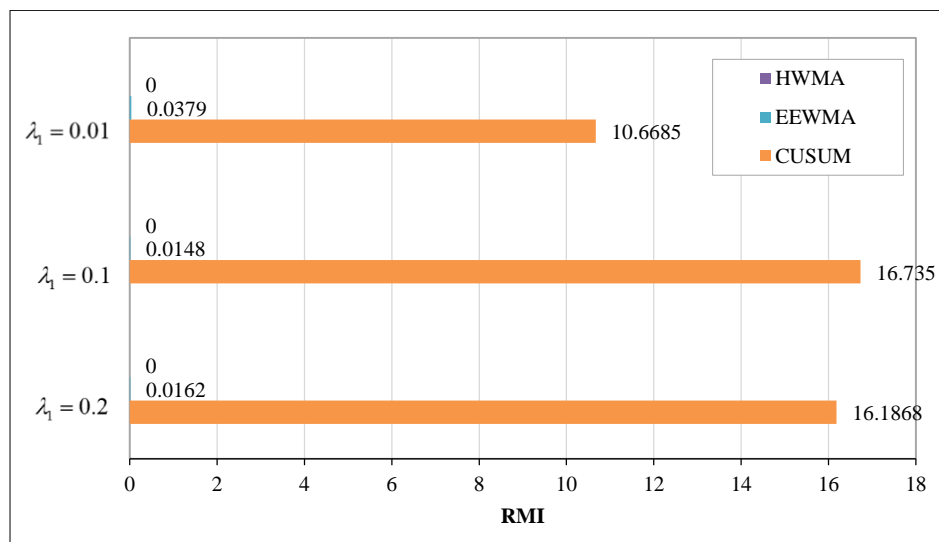
Table 6. The coefficients for the trend AR(p) models using the real-world datasets

Model	AR(1) model				AR(2) model			
Parameters	Coefficient	Std. Error	t-Statistic	p-value	Coefficient	Std. Error	t-Statistic	p-value
AR(1)	0.999	0.002	660.400	0.000	0.742	0.106	7.000	0.000
AR(2)					0.258	0.106	2.432	0.000
RMSE	0.472				0.473			
MAPE	5.389				5.461			

Table 7. One-sample Kolmogorov test for the real-world datasets

Residual of Application	Residual AR(1) model
Exponential parameter	0.1223
One-sample Kolmogorov-Smirnov test	0.635
p-value	0.814

The explicit formula method was used to compare the ARL values for AR(1) on the HWMA, Extended EWMA, and CUSUM control charts; the results are shown in Table 8; it is evident that the results are consistent with those in Tables 4 and 5. The findings indicate that the HWMA control chart exhibits the minimum RMI, AEQL, across all levels of λ . Additionally, the PCI value on the HWMA control chart is 1. The outcomes presented in Table 8 are visually enhanced in Figure 2. In light of this, it can be concluded that the explicit formula for detecting mean process changes on the HWMA control chart is an acceptable alternative for practical applications. Figure 3 also displays the HWMA (Ht), Extended EWMA (Et), and CUSUM (Ct) statistics for the natural gas price corresponding to the AR(1) model. These results indicate that the HWMA control chart can detect a shift for the first time in the first observation, the Extended EWMA control chart can detect a shift for the first time in the third observation, and the CUSUM scheme is identified for the first time in the twelfth observation. The results therefore indicate that the HWMA control chart is preferable to the Extended EWMA and CUSUM control charts for the natural gas price dataset.



(a)

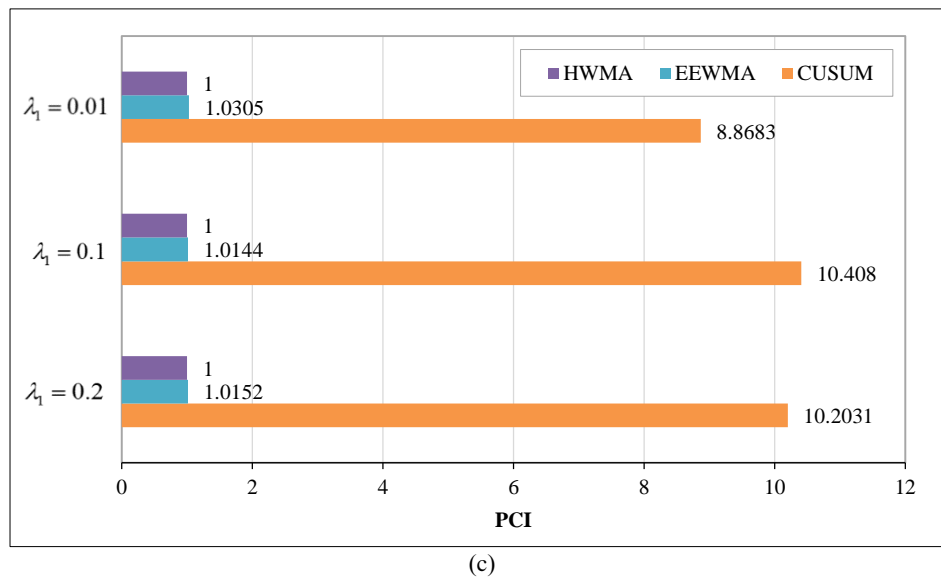
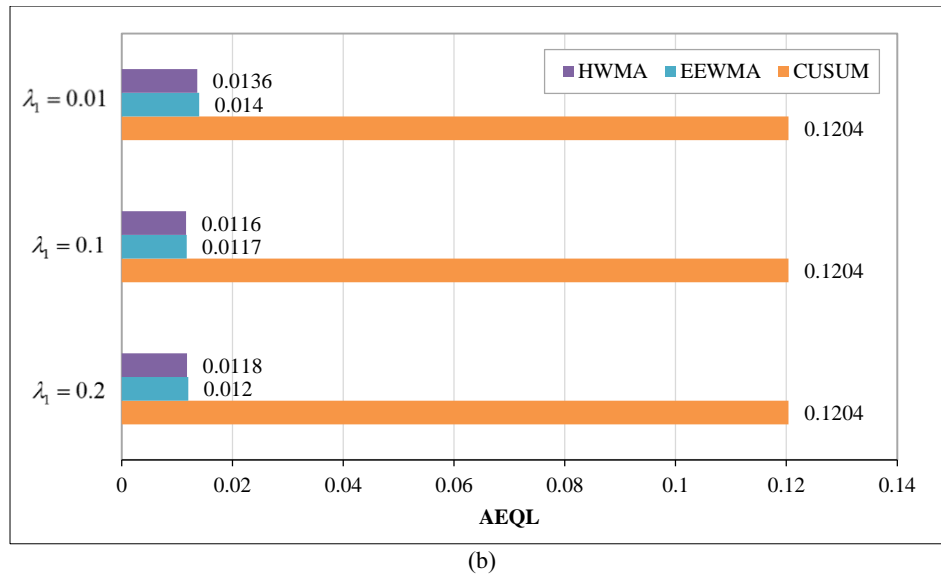
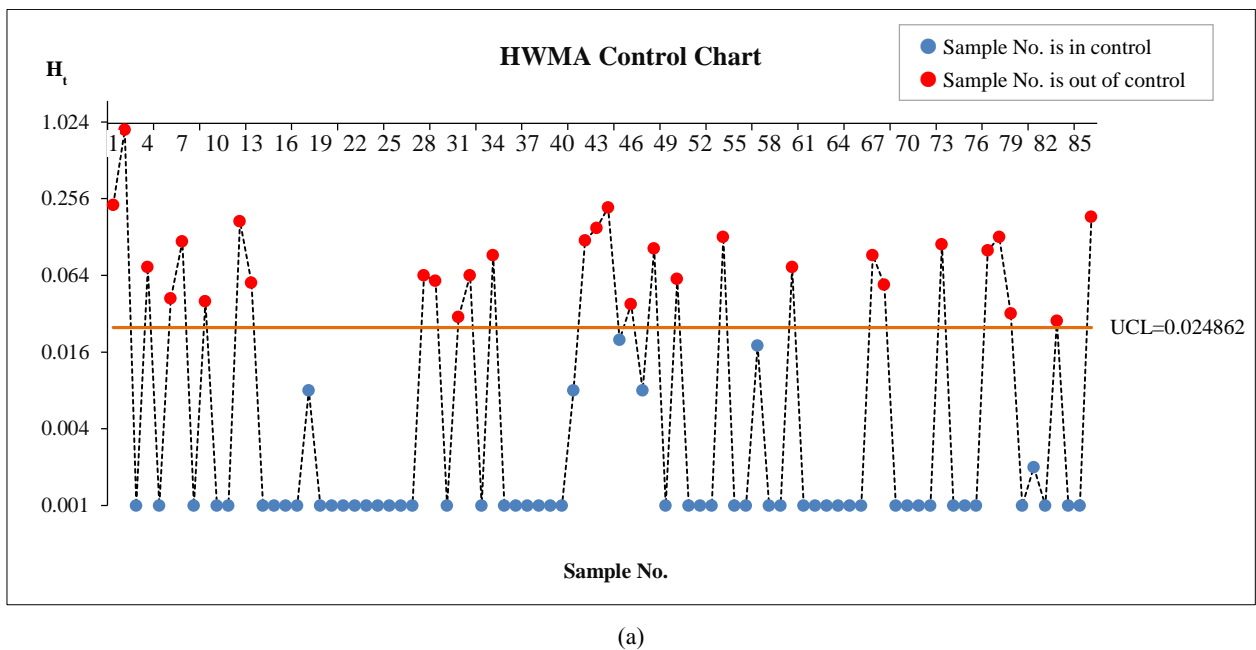
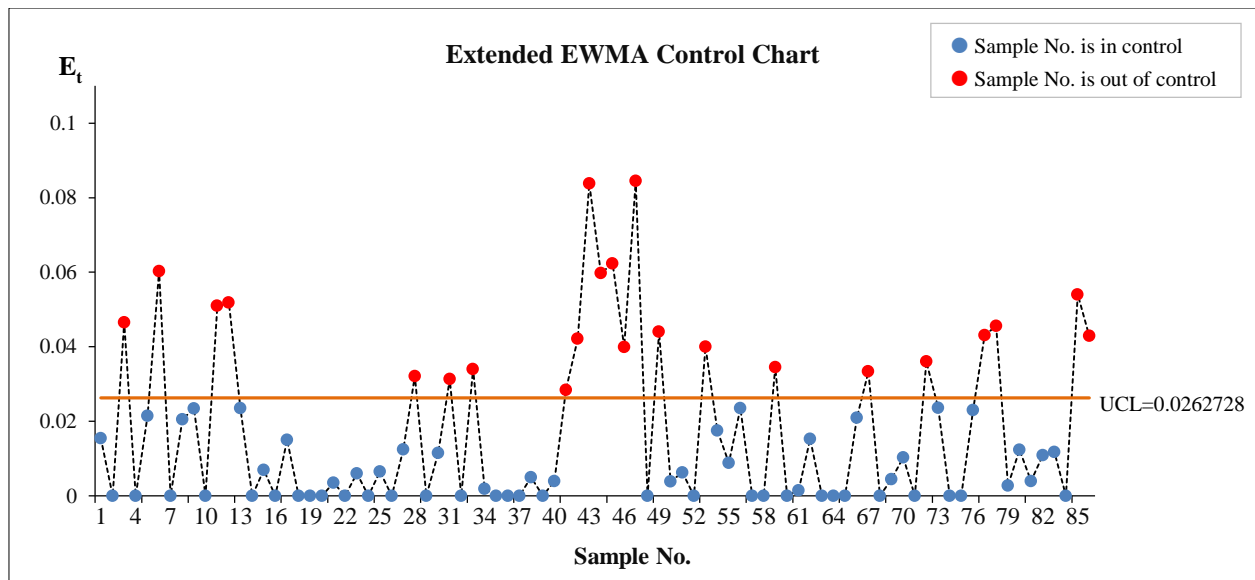
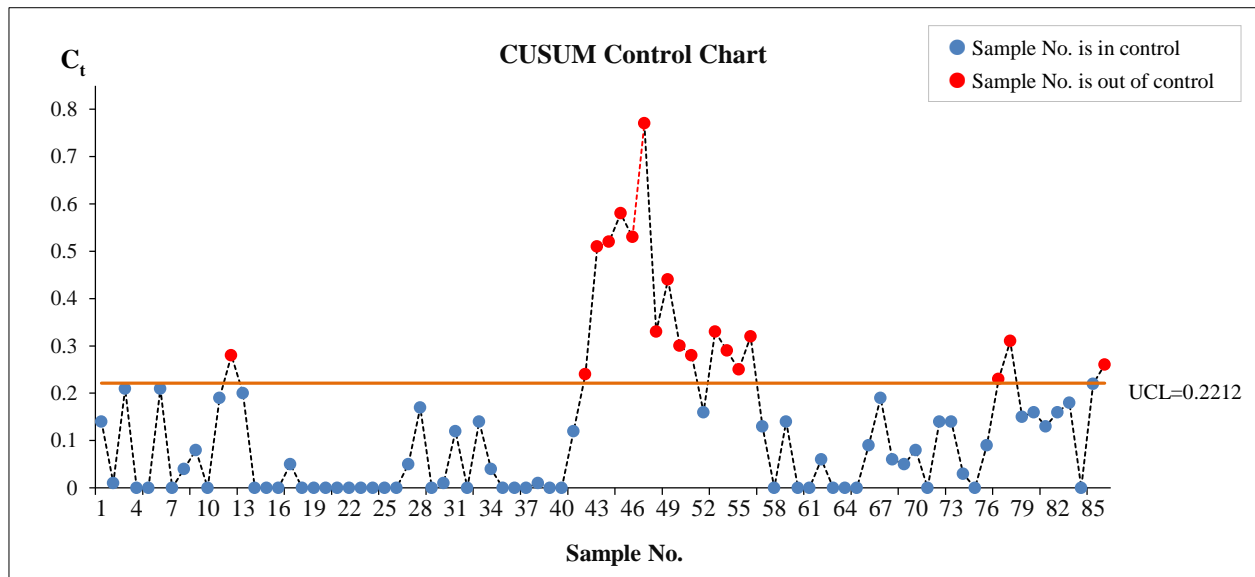


Figure 2. Comparison the RMI, AEQL and PCL values among HWMA, Extended EWMA and CUSUM control charts for AR(1) when (a) $\lambda_1 = 0.01$, (b) $\lambda_1 = 0.1$ and (c) $\lambda_1 = 0.2$





(b)



(c)

Figure 3. The performance comparison of real data among (A) HWMA control chart, (B) Extended EWMA control chart and (C) CUSUM control chart when $\lambda_1=0.2$

Table 8. The ARL of HWMA control chart for AR(1) using explicit formula against Extended EWMA and CUSUM control charts given $\phi_1 = 0.999$ and $\alpha_0 = 0.1223$

δ	λ	Control Chart	$\lambda_1=0.01$			$\lambda_1=0.1$			$\lambda_1=0.2$		
			HWMA	EEWMA $\lambda_2=0.005$	CUSUM a=4.5	HWMA	EEWMA $\lambda_2=0.05$	CUSUM a=4.5	HWMA	EEWMA $\lambda_2=0.05$	CUSUM a=4.5
0.000	UCL	HWMA	0.001128	0.001216	0.2212	0.0118	0.01246988	0.2212	0.024862	0.0262728	0.2212
		ARL ₀	370.0148	370.9366	370.0920	370.0900	370.7941	370.0920	370.8314	370.5368	370.0920
		SDRL ₀	369.5145	370.4363	369.5917	369.5896	370.2938	369.5917	370.3310	370.0364	369.5917
		MRL ₀	256.1280	256.767	256.1815	256.1801	256.6682	256.1815	256.6940	256.4898	256.1815
0.002	UCL	HWMA	68.54312	71.07629	336.1870	39.48426	39.99501	336.1870	40.89710	41.49404	336.1870
		ARL ₁	68.04128	70.57452	335.6866	38.98105	39.49184	335.6866	40.39400	40.99099	335.6866
		SDRL ₁	47.16305	48.91894	232.6803	27.02035	27.37439	232.6803	27.99970	28.41349	232.6803
		MRL ₁	37.95438	39.49063	306.3130	21.38617	21.68080	306.3130	22.17772	22.52451	306.3130
0.004	UCL	HWMA	37.45104	38.98743	305.8126	20.88018	21.17489	305.8126	21.67195	22.01884	305.8126
		ARL ₁	25.95986	27.02477	211.9732	14.47442	14.67868	211.9732	15.02318	15.26361	211.9732
		SDRL ₁									
		MRL ₁									

	ARL ₁	20.22209	21.07776	256.4690	11.57006	11.73811	256.4690	11.99492	12.19157	256.4690
0.008	SDRL ₁	19.71576	20.57168	255.9685	11.05876	11.22699	255.9685	11.48404	11.68087	255.9685
	MRL ₁	13.66738	14.26061	177.4240	7.667960	7.784525	177.4240	7.962644	8.099035	177.4240
	ARL ₁	16.45130	17.15221	235.6180	9.538947	9.679884	235.6180	9.885292	10.04950	235.6180
0.01	SDRL ₁	15.94346	16.6447	235.1175	9.025107	9.166257	235.1175	9.371964	9.536401	235.1175
	MRL ₁	11.05298	11.53896	162.9711	6.258925	6.356714	162.9711	6.499230	6.613156	162.9711
	ARL ₁	8.684650	9.054566	159.7810	5.401260	5.485491	159.7810	5.584750	5.680963	159.7810
0.02	SDRL ₁	8.169363	8.539941	159.2802	4.875690	4.960354	159.2802	5.060107	5.156780	159.2802
	MRL ₁	5.666103	5.922815	110.4048	3.385477	3.444061	110.4048	3.513091	3.579993	110.4048
	ARL ₁	4.719190	4.911566	84.78130	3.284530	3.337927	84.78130	3.382941	3.442405	84.78130
0.04	SDRL ₁	4.189459	4.383139	84.27982	2.739271	2.793534	84.27982	2.839252	2.899611	84.27982
	MRL ₁	2.910778	3.044726	58.41866	1.909164	1.946576	58.41866	1.978104	2.019735	58.41866
	ARL ₁	2.760890	2.860518	34.76150	2.199470	2.234827	34.76150	2.253360	2.291816	34.76150
0.08	SDRL ₁	2.204909	2.306956	34.25785	1.624253	1.661212	34.25785	1.680557	1.720640	34.25785
	MRL ₁	1.541239	1.611416	23.74658	1.143172	1.168423	23.74658	1.181646	1.209057	23.74658
	ARL ₁	2.380200	2.460779	25.11730	1.976790	2.007815	25.11730	2.021350	2.054885	25.11730
0.10	SDRL ₁	1.812499	1.895958	24.61222	1.389571	1.422500	24.61222	1.436839	1.472300	24.61222
	MRL ₁	1.271932	1.329121	17.06107	0.983246	1.005636	17.06107	1.015392	1.039531	17.06107
	ARL ₁	1.647260	1.68883	9.108460	1.516840	1.537068	9.108460	1.541582	1.563148	9.108460
0.20	SDRL ₁	1.032572	1.078571	8.593927	0.885417	0.908575	8.593927	0.913725	0.938235	8.593927
	MRL ₁	0.742032	0.772914	5.960214	0.643799	0.659194	5.960214	0.662620	0.678948	5.960214
	RMI	0	0.0379	10.6685	0	0.0148	16.7350	0	0.0162	16.1868
	AEQL	0.0136	0.0140	0.1204	0.0116	0.0117	0.1204	0.0118	0.0120	0.1204
	PCI	1	1.0305	8.8683	1	1.0144	10.4080	1	1.0152	10.2031

5. Conclusion

In this research, for an AR process with exponential white noise on an HWMA control chart, the ARL is proven and compared with the NIE technique. The results of the comparison showed that the ARL values obtained using the explicit formula and the NIE method were similar. Moreover, the existence and uniqueness of ARL derivatives according to clear formulas have been proven. In addition, the SDRL and MRL values were studied, which found that the results were in the same direction as the ARL values.

Taking into account the variation of the parameters at different levels, the performance of the HWMA, Extended EWMA, and CUSUM control charts is studied by comparing the ARL values when the process is out of control. The RMI, AEQL, and PCI values were used to compare their performances on HWMA, Extended EWMA, and CUSUM control charts. The results indicated that the HWMA control chart exhibited lower RMI and AEQL values in comparison to the Extended EWMA and CUSUM control charts. Additionally, the HWMA control chart maintained a PCI value of 1. In conclusion, the HWMA control chart exhibits the most significant efficiency. Additionally, the price of natural gas is utilized as actual data to evaluate the HWMA control chart's performance. The benefit of this application is that it provides these results and conceptions for developing strategies to identify price-level changes. Natural gas is generally traded on commodity exchanges based on supply and demand forces in these markets.

Consequently, if we use a control chart to monitor price fluctuations, this can be used as a guide by traders and investors to make trading decisions based on forecasts of future price movements by combining fundamental research, which looks at supply and demand factors, with technical analysis, which looks at graph patterns and historical price data. In conclusion, the findings show that the HWMA control chart outperformed the Extended EWMA and CUSUM control charts for all change magnitudes. Furthermore, the outcomes from the simulation study and a real-world situation concerning the price of natural gas agreed. While there is potential for the explicit formula derivation of the ARL to be implemented in other situations, it is limited to the AR model and exponential white noise. Alternative methods for calculating the ARL value, such as the NIE or Markov chain approach, may be required if the analyzed data contains additional white noise patterns. Finally, further research will be undertaken to apply the explicit ARL formulas displayed on the HWMA chart to other real-world data models, such as ARIMA and ARMA. In addition, we will apply this technique to derive the explicit formula for new control charts in order to enhance their ability to detect change in various situations.

6. Declarations

6.1. Author Contributions

Conceptualization, Y.A. and S.S.; methodology, R.S.; software, Y.A.; validation, R.S., S.S., and Y.A.; formal analysis, R.S.; investigation, S.S.; resources, Y.A.; data curation, Y.A.; writing—original draft preparation, Y.A.; writing—review and editing, Y.A.; visualization, R.S.; supervision, Y.A.; project administration, S.S.; funding acquisition, Y.A. All authors have read and agreed to the published version of the manuscript.

6.2. Data Availability Statement

The data presented in this study are available in the article.

6.3. Funding

This research was funded by Thailand Science Research and Innovation Fund (NSRF), and King Mongkut's University of Technology North Bangkok with Contract no. KMUTNB-FF-67-B-11.

6.4. Institutional Review Board Statement

Not applicable.

6.5. Informed Consent Statement

Not applicable.

6.6. Declaration of Competing Interest

The authors declare that they have no known competing financial interests or personal relationships that could have appeared to influence the work reported in this paper.

7. References

- [1] Shewhart, W. A. (1932). The Economic Control of Quality of Manufactured Product. *Journal of the Royal Statistical Society*, 95(3), 546-549. doi:10.2307/2342413.
- [2] Page, E. S. (1954). Continuous Inspection Schemes. *Biometrika*, 41(1/2), 100. doi:10.2307/2333009.
- [3] Roberts, S. W. (1959). Control Chart Tests Based on Geometric Moving Averages. *Technometrics*, 1(3), 239. doi:10.2307/1266443.
- [4] Crowder, S. V. (1987). A simple method for studying run – length distributions of exponentially weighted moving average charts. *Technometrics*, 29(4), 401–407. doi:10.1080/00401706.1987.10488267.
- [5] Lucas, J. M., & Saccucci, M. S. (1990). Exponentially weighted moving average control schemes: Properties and enhancements. *Technometrics*, 32(1), 1–12. doi:10.1080/00401706.1990.10484583.
- [6] Naveed, M., Azam, M., Khan, N., & Aslam, M. (2018). Design of a Control Chart Using Extended EWMA Statistic. *Technologies*, 6(4), 108. doi:10.3390/technologies6040108.
- [7] Abbas, N. (2018). Homogeneously weighted moving average control chart with an application in substrate manufacturing process. *Computers and Industrial Engineering*, 120, 460–470. doi:10.1016/j.cie.2018.05.009.
- [8] Riaz, M., Ahmad, S., Mahmood, T., & Abbas, N. (2022). On Reassessment of the HWMA Chart for Process Monitoring. *Processes*, 10(6). doi:10.3390/pr10061129.
- [9] Fellag, H., & Ibazizen, M. (2001). Estimation of the first-order autoregressive model with contaminated exponential white noise. *Journal of Mathematical Sciences*, 106(1), 2652–2656. doi:10.1023/A:1011318515549.
- [10] Champ, C. W., & Ritrdon, S. E. (1991). A Comparison of the Markov Chain and the Integral Equation Approaches for Evaluating the Run Length Distribution of Quality Control Charts. *Communications in Statistics - Simulation and Computation*, 20(1), 191–204. doi:10.1080/03610919108812948.
- [11] Sukparungsee, S., & Areepong, Y. (2017). An explicit analytical solution of the average run length of an exponentially weighted moving average control chart using an autoregressive model. *Chiang Mai Journal of Science*, 44(3), 1172–1179.
- [12] Sunthornwat, R., Areepong, Y., & Sukparungsee, S. (2018). Average run length with a practical investigation of estimating parameters of the EWMA control chart on the long memory AFRIMA process. *Thailand Statistician*, 16(2), 190–202.
- [13] Peerajit, W., Areepong, Y., & Sukparungsee, S. (2018). Numerical integral equation method for ARL of CUSUM chart for long-memory process with non-seasonal and seasonal ARFIMA models. *Thailand Statistician*, 16(1), 26–37.

- [14] Supharakonsakun, Y., Areepong, Y., & Sukparungsee, S. (2020). The exact solution of the average run length on a modified EWMA control chart for the first-order moving-average process. *ScienceAsia*, 46(2023), 109-118. doi:10.2306/scienceasia1513-1874.2020.015.
- [15] Supharakonsakun, Y. (2021). Statistical design for monitoring process mean of a modified EWMA control chart based on autocorrelated data. *Walailak Journal of Science and Technology*, 18(12), 19813. doi:10.48048/wjst.2021.19813.
- [16] Phanyaem, S. (2022). Explicit Formulas and Numerical Integral Equation of ARL for SARX(P,r)L Model Based on CUSUM Chart. *Mathematics and Statistics*, 10(1), 88–99. doi:10.13189/ms.2022.100107.
- [17] Petcharat, K. (2022). The Effectiveness of CUSUM Control Chart for Trend Stationary Seasonal Autocorrelated Data. *Thailand Statistician*, 20(2), 475–488.
- [18] Phanthuna, P., & Areepong, Y. (2022). Detection Sensitivity of a Modified EWMA Control Chart with a Time Series Model with Fractionality and Integration. *Emerging Science Journal*, 6(5), 1134–1152. doi:10.28991/ESJ-2022-06-05-015.
- [19] Peerajit, W., & Areepong, Y. (2023). Alternative to Detecting Changes in the Mean of an Autoregressive Fractionally Integrated Process with Exponential White Noise Running on the Modified EWMA Control Chart. *Processes*, 11(2), 503. doi:10.3390/pr11020503.
- [20] Silpakob, K., Areepong, Y., Sukparungsee, S., & Sunthornwat, R. (2023). A New Modified EWMA Control Chart for Monitoring Processes Involving Autocorrelated Data. *Intelligent Automation and Soft Computing*, 36(1), 281–298. doi:10.32604/iasc.2023.032487.
- [21] Peerajit, W. (2023). Developing Average Run Length for Monitoring Changes in the Mean on the Presence of Long Memory under Seasonal Fractionally Integrated MAX Model. *Mathematics and Statistics*, 11(1), 34–50. doi:10.13189/ms.2023.110105.
- [22] Karoon, K., Areepong, Y., & Sukparungsee, S. (2023). Trend Autoregressive Model Exact Run Length Evaluation on a Two-Sided Extended EWMA Chart. *Computer Systems Science and Engineering*, 44(2), 1143–1160. doi:10.32604/csse.2023.025420.
- [23] Karoon, K., Areepong, Y., & Sukparungsee, S. (2023). On the Performance of the Extended EWMA Control Chart for Monitoring Process Mean Based on Autocorrelated Data. *Applied Science and Engineering Progress*, 16(4), 6599. doi:10.14416/j.asep.2023.01.004.
- [24] Peerajit, W. (2023). Statistical Design of a One-sided CUSUM Control Chart to Detect a Mean Shift in a FIMAX Model with Underlying Exponential White Noise. *Thailand Statistician*, 21(2), 397–420.
- [25] Peerajit, W. (2023). Accurate Average Run Length Analysis for Detecting Changes in a Long-Memory Fractionally Integrated MAX Process Running on EWMA Control Chart. *WSEAS Transactions on Mathematics*, 22, 514–530. doi:10.37394/23206.2023.22.58.
- [26] Sunthornwat, R. (2023). Analytical Explicit Formulas of Average Run Length of Homogenously Weighted Moving Average Control Chart Based on a MAX Process. *Symmetry*, 15(12), 2112. doi:10.3390/sym15122112.
- [27] Brahmasrene, T., Huang, J. C., & Sissoko, Y. (2014). Crude oil prices and exchange rates: Causality, variance decomposition and impulse response. *Energy Economics*, 44, 407–412. doi:10.1016/j.eneco.2014.05.011.
- [28] Fonseca, A., Ferreira, P. H., Do Nascimento, D. C., Fiaccone, R., Ulloa-Correa, C., García-Piña, A., & Louzada, F. (2021). Water particles monitoring in the Atacama Desert: SPC approach based on proportional data. *Axioms*, 10(3), 154. doi:10.3390/axioms10030154.
- [29] Tang, A., Castagliola, P., Sun, J., & Hu, X. (2019). Optimal design of the adaptive EWMA chart for the mean based on median run length and expected median run length. *Quality Technology and Quantitative Management*, 16(4), 439–458. doi:10.1080/16843703.2018.1460908.
- [30] Alevizakos, V., Chatterjee, K., & Koukouvinos, C. (2021). The triple exponentially weighted moving average control chart. *Quality Technology and Quantitative Management*, 18(3), 326–354. doi:10.1080/16843703.2020.1809063.